Pharmaceutical Research, Vol. 26, No. 3, March 2009 (© 2008)
DOI: 10.1007/s11095-008-9804-z

Research Paper

Nanocomposite Degradable Hydrogels: Demonstration of Remote Controlled Degradation and Drug Release

Ashley M. Hawkins,[1] Nitin S. Satarkar,[1] and J. Zach Hilt[1,2]

Received September 19, 2008; accepted December 1, 2008; published online January 1, 2009

Purpose. To demonstrate remote controlled degradation of degradable nanocomposite hydrogels by application of an alternating magnetic field (AMF). Further, it was desired to study the AMF effect on the drug release properties of these systems.
Methods. Degradable nanocomposite hydrogels were synthesized by incorporating iron oxide nanoparticles into a degradable hydrogel that exhibited temperature dependent degradation. Heating, degradation, and drug release studies were conducted by application of an AMF to determine if modulation of degradation and drug release could be attained.
Results. Hydrogels were successfully prepared, shown to have temperature dependent degradation, and shown to heat when exposed to the AMF. The degradation rate of the exposed samples was demonstrated to be higher than control samples, thus modulation of degradation was obtained. The release of a model drug from the system was modulated by exposure to the AMF.
Conclusions. This is the first demonstration of remote controlled degradation using an AMF stimulus. Here, the proof of the concept has been presented, and there is great potential to enhance this effect through various methods. The ability to remotely control degradation of an implanted device opens a new area of improved medical devices.

KEY WORDS: degradable polymers; drug release; hydrogels; nanocomposite; remote control.

INTRODUCTION

Recent advancements in biology, medicine, and engineering have led to the increased use of biodegradable polymers in areas ranging from drug delivery to tissue engineering (1). Hydrogels are hydrophilic crosslinked polymer chain networks that can provide "stealth" properties to the system as well as control over the stability, mechanical properties, and degradation profile making them desirable for medical applications (2–5). In particular, they are attractive for *in vivo* applications as the hydrophilicity and hydrated state can be similar to that of natural tissue, and there is potential to form hydrogels *in situ* (6–8). Biodegradable hydrogels have recently attracted much attention and have been applied as a biomaterial for tissue engineering and/or drug release purposes as no additional procedures are necessary to remove the remaining matrix after application (3,4). Hubbell and others developed one of the first biodegradable hydrogels by incorporating hydrolytically labile bonds into the structure (9). In the last several years, a vast array of novel systems has been developed. For example, a recent paper by Anderson *et al.* has created a combinatorial library of 120 macromers that form photocrosslinkable degradable hydrogel systems (10,11). For previously developed degradable polymer systems, the degradation rate is preprogrammed and not adjustable after implantation of the materials or device. Here, a degradable hydrogel nanocomposite has been developed with degradation properties that can be controlled by an external stimulus. In recent years, several non-degradable nanocomposite hydrogel systems have been developed for remote controlled (RC) applications. For example, gold nanoshells have been remotely heated by the exposure to light, especially near-infrared (12,13) and iron oxide nanoparticles have been heated through application of an alternating magnetic field (AMF) (14–17). In the case of iron oxide nanoparticles, the nanoparticles can be heated through several mechanisms including hysteresis, Neel and Brownian relaxation, and frictional losses in a viscous fluid (18).

In this study, a degradable hydrogel with temperature sensitive degradation was fabricated with iron oxide nanoparticles dispersed throughout the matrix. Upon application of an external magnetic field, the nanoparticles heat, and increase the rate of degradation on the network. This is the first demonstration of RC degradation using an AMF stimulus. Here, the proof of the concept has been presented, and there is great potential to enhance this effect through various methods. (*e.g.*, choice of a more temperature dependent polymer or increasing the intensity of the AMF).

[1] Department of Chemical and Materials Engineering, University of Kentucky, 177 F. Paul Anderson Tower, Lexington, KY 40506-0046, USA.
[2] To whom correspondence should be addressed. (e-mail: hilt@engr.uky.edu)

The ability to remotely control degradation of an implanted device opens a new area of improved medical devices. For drug delivery applications, this could enable new methods of delivering time dependent drugs to patients and for modulating the dosage of drug if the patient's needs change after the device's implantation. This technology could also be utilized in tissue engineering scaffolds to provide the ability to modulate the degradation profile.

In demonstrating remote control over drug release, several requirements had to first be met: the gels had to display a temperature dependent degradation, the nanoparticles had to heat the gels, and finally the exposure to the field had to show some effect on the degradation and thus drug release of the nanocomposite. This paper outlines the specific studies and processes that were followed to ultimately demonstrate that the nanocomposite hydrogels can be a useful tool in controlled release drug delivery devices.

MATERIALS AND METHODS

Materials

Diethylene glycol diacrylate was purchased from Polysciences, Inc. Iron oxide (Fe_3O_4, magnetite) nanoparticles with 20–30 nm diameter (~0.2% Surfactant PVP coated) were purchased from Nanostructured and Amorphous Materials Inc. 3-morpholinopropylamine, ammonium persulphate, phosphate buffer saline solution (PBS), ammonium persulphate (APS), and tetramethylethylene diamine (TEMED) were purchased from Sigma. Green tea polyphenols (GTP) was purchased from LKT Laboratories. All materials were used as received.

Methods

Macromer Synthesis

Here, macromer synthesis was carried out in accordance with the prior paper (10). The system chosen was for ease of the study. Diethylene glycol diacrylate and 3-morpholinopropylamine were weighed out to the desired molar ratio, for this research ratios of 1.3, 1.6, and 2.0 diacrylate to amine were used, the mixture was reacted overnight in a sealed round-bottom flask with magnetic stirrer Fig. 1. A heating mantle was used to keep the reaction temperature stable at 85°C. When complete, the solution was pipetted out and placed in an amber vial stored at 4°C.

FTIR Analysis

IR analysis was utilized to analyze the chemical composition of the amines, diacrylate, macromers, and polymerized gels. The IR spectra were obtained using the attenuated total reflectance (ATR) setup of fourier transform infrared spectrometer (Varian 700e FTIR). The macromer solutions to be tested were pipetted onto the ATR crystal, and the spectra were collected.

Gel Permeation Chromatography (GPC)

GPC (Shimadzu) was used to determine the average molecular weight and polydispersity index of the macromer solution. For the systems studied, the macromer was mixed with tetrahydrofuran (THF) to a concentration of 5 mg/mL. The distribution of the molecular weights present was obtained.

Viscometry

The viscosity of the macromers was measured using a Brookfield cone and plate viscometer. The results provide another representation of the molecular weight of the polymer chains present, as higher molecular weight systems have a higher viscosity than their lower molecular weight counterparts.

Degradable Hydrogel Nanocomposite Synthesis

Free radical polymerization was used to create the nanocomposite gels for further study. The macromer chains are terminated by vinyl groups which react to form the hydrogel system. For this portion and the remaining parts of the experimentation the macromer with the 1.3 mol diacrylate to amine ratio was used. The polymerization was carried out between glass plates separated by 1 mm thick Teflon spacers.

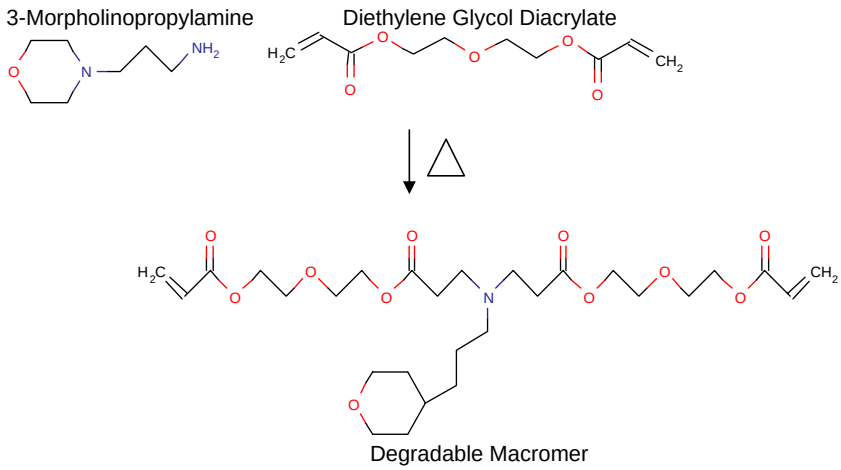

Fig. 1. Macromer synthesis. The diacrylate and amine were mixed in the desired molar ratio at 85°C overnight.

Approximately 2 g of the 1.3 diacrylate to amine ratio macromer was weighed and sonicated with a mixture of 5 wt.% iron oxide nanoparticles and 50 wt.% ethanol (both percentages based upon macromer weight). Separately, 1.5 wt.% APS (based on macromer weight) was mixed with 200 μL DI water until dissolved. Finally, the APS solution and 2.25 wt.% TEMED (based on macromer weight) were added simultaneously to the macromer solution and sonicated for approximately 20 s before transferring into the glass plate assembly. The plates were allowed to sit at room temperature overnight to ensure complete polymerization. Once removed from the plates, the gels were washed for two 30 s time periods in de-ionized water. No visible nanoparticle leaching occurred during the washing step, thus indicating that the particles were physically entrapped within the gel. Samples with 11.45 mm diameter were cut and freeze-dried to remove any residual water. Pure control hydrogels were synthesized using the same procedure with no addition of nanoparticles.

Quantification of Remote Heating

To measure the heating that occurs due to the iron oxide nanoparticles, the gels were exposed to the AMF, and the surface temperature was recorded by an infrared camera (AGEMA Thermovision 470). Samples of the gel in the dry state were placed in a glass Petri dish set on top of the solenoid of the induction power supply (Taylor-Winfield 3 kW). The solenoid dimensions were 32 mm length with a radius of 10 mm, thus field strength at the top of the coils is calculated to be 29.13 gauss and the frequency is 293 KHz.

Demonstration of Temperature Dependent Degradation

The samples were degraded at several temperatures, and the mass loss was recorded. After freeze-drying, samples were weighed to record the initial mass and immediately placed into centrifuge tubes with PBS (ph=7.4) equilibrated at 25°C, 37°C, and 55°C. Every 45 min samples were taken out of the PBS and taken to the freeze-dryer. This method was used to study the degradation, since it preserves the samples after removal from the water baths by preventing further degradation.

RC Degradation Studies

Composite gel samples were weighed and placed into PBS solution in a 15 mL centrifuge tube. AMF exposure was applied for 5 min times at 0, 10, 20, 40, 50, 60, 80, 90, and 100 min into the degradation. For degradation and the drug release studies, the centrifuge tube was placed inside the solenoid of the induction heating supply so as the gel is in the center of the coils, the field frequency and strength at this location were 293 KHz and 51.75 gauss, respectively. When not in the field, the samples were kept in the 37°C water bath. The PBS solution was changed every 20 min to maintain infinite sink conditions. At 60, 80, and 100 min, samples were taken out and freeze dried to analyze the fraction of mass remaining.

Drug Imbibition & Release Studies

After freeze drying, gels were imbibed with the model drug using dimethyl sulfoxide (DMSO) as the solvent. Green tea polyphenols were chosen as the model drug for their large structure, high solubility in DMSO, and prominent UV–vis peak.

For the drug imbibition process, green tea polyphenols were dissolved in DMSO to obtain a concentration of 25 mg/mL. Each hydrogel sample was weighed and placed into this solution, imbibed for 48 h, then removed and allowed to dry in the fume hood overnight.

Drug imbibed samples were washed for two 30 s time periods in room temperature PBS to remove surface adsorbed drug and avoid a large initial burst effect. Samples were then placed in 37°C PBS in a 15 mL centrifuge tube. The control samples and field exposed samples were placed in the 37°C bath. Field exposed samples were placed in the induction heating instrument solenoid for the same dosing schedule as outlined in the field degradation section. For data collection, the PBS supernatant was removed from the samples and replaced with 37°C PBS every 20 min. The final time point was taken after allowing the sample to completely degrade. The PBS remaining was filtered through a 0.2 μm filter. The supernatant was analyzed with UV–Vis and the peak at ~271 nm was recorded.

RESULTS

Macromer Characterization

The results found in the GPC and viscosity studies are outlined in Table I in the "Appendix". As the diacrylate to amine ratio increased the molecular weight of the macromer chains decreased. This is evident in the number average molecular weights (M_n) and the weight average molecular weights (M_w). The viscosity also provides a measure of the molecular weight. The large molecular weight macromers were observed to be much more viscous than the higher ratio, smaller molecular weight systems. FTIR analysis shown in Fig. 2 also shows a difference in carbon–carbon double bond peak intensity at 1,636 cm^{-1}. The lower molecular weight systems (diacrylate to amine ratio of 2.0) have many more chains and thus more vinyl end groups present, creating a larger absorbance in the carbon–carbon double bond range as opposed to the larger molecular weight systems (diacrylate to amine ratio of 1.3).

Quantification of Remote Heating

The surface temperature of the gels in the dry state was measured while the gels sat on top of the solenoid. Fig. 3 plots the surface temperature of the gel *versus* time for the 5 min exposure. The heating data does demonstrate that the gels heat due to the nanoparticles and this heating can reach values significantly higher than the pure gel samples. The pure gels also demonstrate some slight heating which can be attributed to some resistive heating that occurs. For the drug release and field degradation studies the gels were immersed in PBS solution for the tests, which provides a heat sink for the gel, and the sample is located in the center of the solenoid

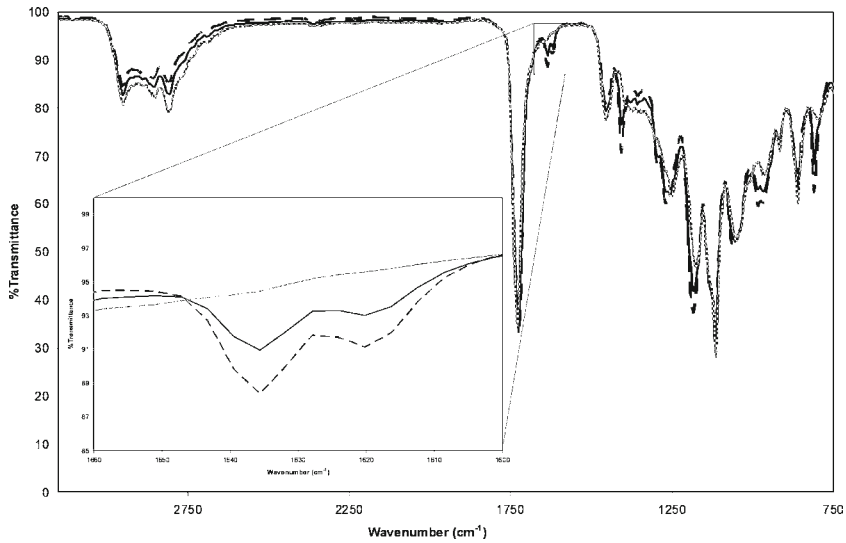

Fig. 2. Macromer FTIR spectra. *Inset* of the range between 1,650 and 1,600, the range of the carbon double bond peak. 1.2 D:A ▭▭▭▭▭▭ , 1.6 D:A ▭▭▭▭▭▭ , 2.0 D:A ▭▭▭▭▭▭ .

as opposed to the top, resulting in a stronger AMF, thus the temperature can be significantly different than those measured.

Demonstration of Temperature Dependent Degradation

The temperature of the system during degradation can have a large effect on the rate of degradation. The pure and particle samples are plotted separately in Fig. 4. Both systems had their slowest degradation at 25°C and the fastest at 55°C. It was observed that the particles appear to slow the degradation. When plotted as the fraction of mass remaining *versus* time the graphs appear linear thus allowing reaction kinetics to be applied to the hydrolysis for determining the values of activation energy ($-E_a$) and the rate constant (k). Because of the linear nature of the graphs, degradation was assumed to have zero-order kinetics, therefore:

$$[A] + [H_2O] \xrightarrow{\text{yields}} \text{Degradation Products}$$
$$\frac{d[A]}{dt} = -k$$
$$[A] - [A]_o = -kt$$

Thus the slope of the concentration *vs.* time curve was determine for all temperatures (T) to give the value of the reaction constant k. The Arrhenius equation states that:

$$k = Ae^{-E_a/RT}$$

Therefore,

$$In(k) = \frac{-E_a}{R}\frac{1}{T} + In(A)$$

So for each sample type (pure or particle), rate constant and temperature data was used to find the $-E_a/R$ values. For the pure and particle systems, the k values are reported in Tables II and III in the "Appendix". The particle gels were found to have an E_a/R value of 4,736 K, and the pure gels had a value of 4,189 K. It was observed that the particle gels have a higher activation energy for the hydrolysis, thus a slower degradation rate as compared to the pure gels. This is most likely due to a chemical or physical interaction that stabilizes the gel structure, more studies are needed to determine the exact cause.

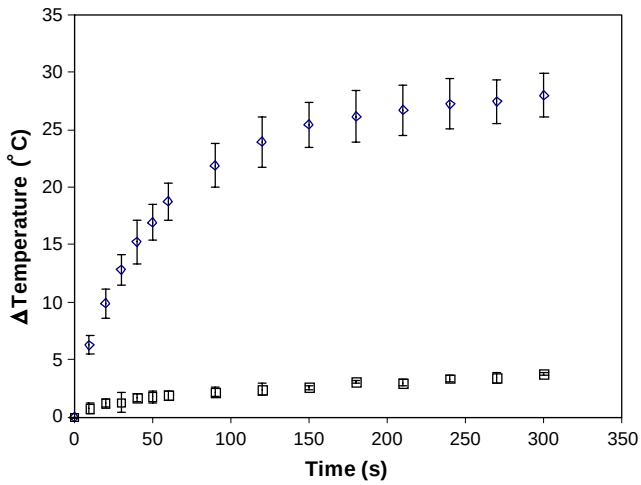

Fig. 3. ΔT values representing the change in surface temperature of the pure (*square*), and 5 wt.% (based on macromer) particle loaded gels (*diamond*). Samples placed on *top* of solenoid. N=3±1 standard deviation.

Degradation in Samples Exposed to AMF

In order to determine if the AMF exposure increased the degradation rate, the degradation in the field was analyzed. The results shown in Fig. 5 demonstrate that the heating of the gels by the field leads to an increase in degradation rate. The plot is still linear with the slope greater than that of the particle gels kept at 37°C. Based on the previous degradation data, the field degradation plot falls between the 37°C and 55°C points, therefore, the field exposure for the intermittent

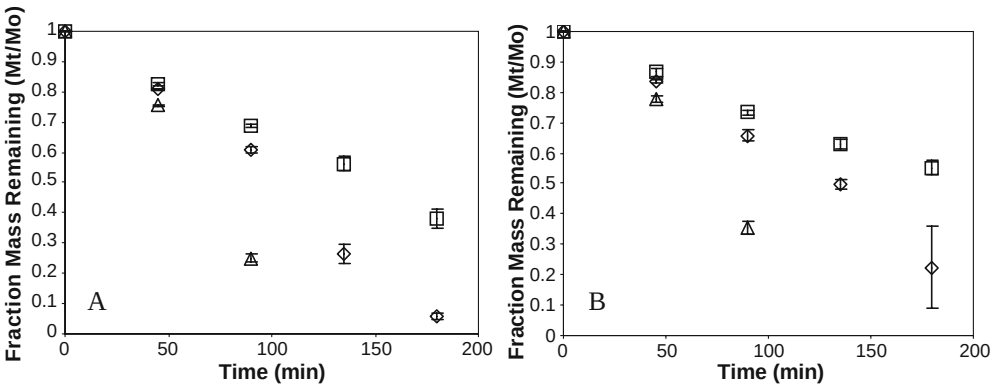

Fig. 4. Temperature dependent degradation. **A** Samples of pure gels at 25°C (*square*), 37°C (*diamond*), 55°C (*triangle*), and **B** particle gels at 25°C (*square*), 37°C (*diamond*), and 55°C (*triangle*). $N=3\pm1$ standard deviation.

time periods appears to have the same effect as if the gel was exposed to a constant high temperature. For future *in vivo* applications, this is desirable as the local temperature near the implant would need to be elevated for staggered amounts of time, as opposed to a continuous elevation in temperature that could harm healthy tissue.

Demonstration of Remote Controlled Drug Release

The final analysis of the system was to analyze the effect the heating of the AMF on the rate of a model drug released from the system. The resulting data is plotted in Figs. 6 and 7, where both pure and particle loaded gels were exposed to the field, and the results were compared to the control samples that were kept in the 37°C water bath. The pure samples show the AMF-exposed drug release is actually slightly below that of the control. This is most likely due to the cooling experienced by the gel and surrounding PBS when taken out of the bath and placed in the field. The particle-loaded gels on the other hand have a very different result as the AMF-exposed samples were consistently above that of the control, and the difference increased at later time points. The AMF exposure is shown to have an effect on the drug release, both compensating for the cooling experienced by taking the sample out of the bath and placing in the field, as well as increasing the temperature of the sample leading to increased degradation and therefore drug release. The most significant result, though difficult to show in this experiment, was the final time point of the drug release. As was shown in the AMF exposed degradation study, the AMF-exposed particle-loaded gel degrades much faster than the control. As was observed in the drug release, the samples from the field were far too degraded to take an accurate supernatant samples at 120 min, however the control samples allowed for this time point. The field exposed samples were completely degraded by 130 min, and the control samples took longer to completely degrade.

DISCUSSION

The remote control over drug release was demonstrated, indicating the potential for this novel system to be used in an

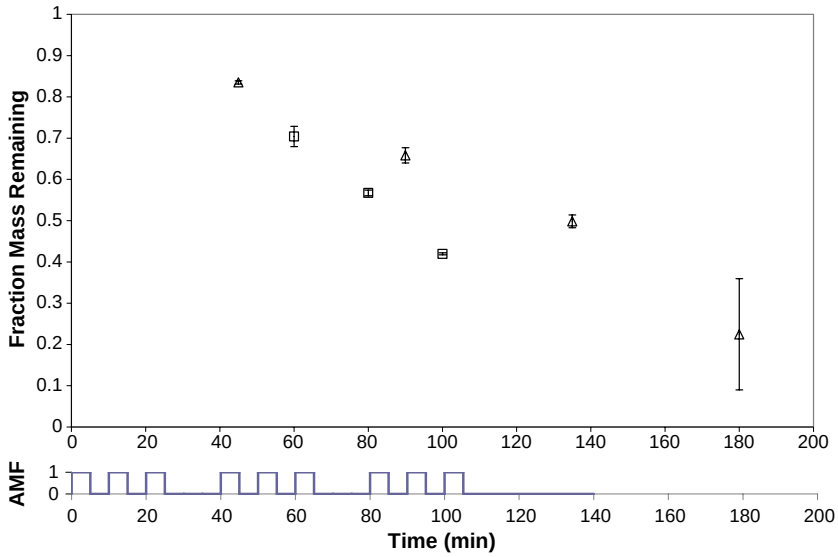

Fig. 5. Field degradation study demonstrating that field exposure increases the rate of hydrogel degradation. Particle samples in 37°C water bath (*triangle*), and particle loaded samples exposed to EMF (*square*). *Lower graph* represents the field dosing schedule, *1* on, *0* off. $N=3$, ± 1 standard deviation.

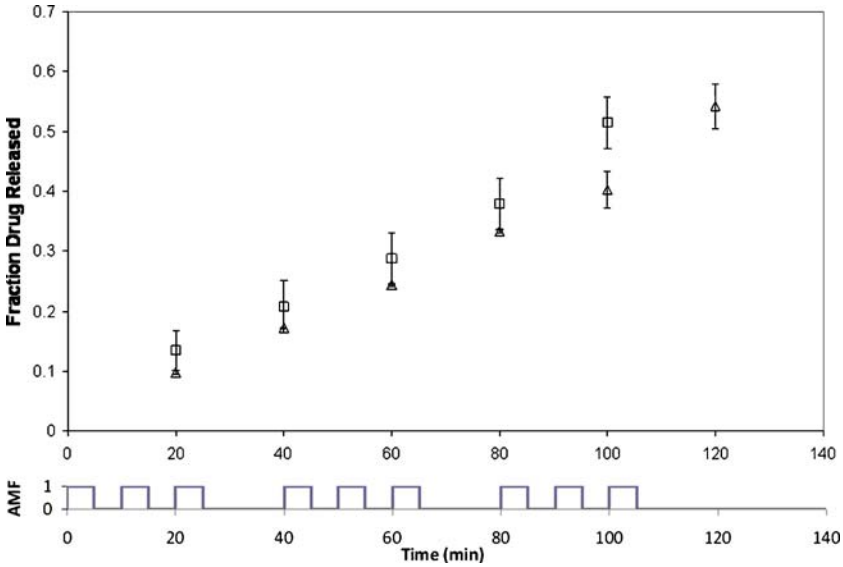

Fig. 6. Particle-loaded drug release profile indicating an shift in the drug release profile of particle loaded gels exposed to the AMF. Particle control samples kept at 37°C (*triangle*), compared to the particle-loaded EMF exposed samples (*square*). *Lower graph* represents the field dosing schedule, *1* on, *0* off. $N=3\pm1$ standard deviation.

in vivo environment to allow external control over an implanted drug delivery device. There are several options for further increasing the effect of the AMF. To increase the effect of the field, longer dosing periods can be used, as well as increasing the intensity and strength of the field. Longer field dosing time periods can keep the temperature of the system elevated for longer times, therefore increasing the degradation. A stronger field source could be used, this would cause the particles themselves to heat more, thus increasing the gel temperature. This alternative however would be restricted in *in vivo* applications as the temperature of the gels must be controlled as well as the body's exposure to the AMF. Other possible avenues to pursue are with the polymer itself. Systems with greater temperature dependent degradation would be affected much more by the same amount of heating and the degradation rate would increase. The polymer chemistry also plays a major role in the degradation rate and time period of the system. For this particular study, a very fast degrading system was used for feasibility in experimentation. This system however, would not be very beneficial for *in vivo* application because of the fast degradation timeframe. Longer degrading systems would need to be used that could respond to the AMF differently, and show a better control over the drug release.

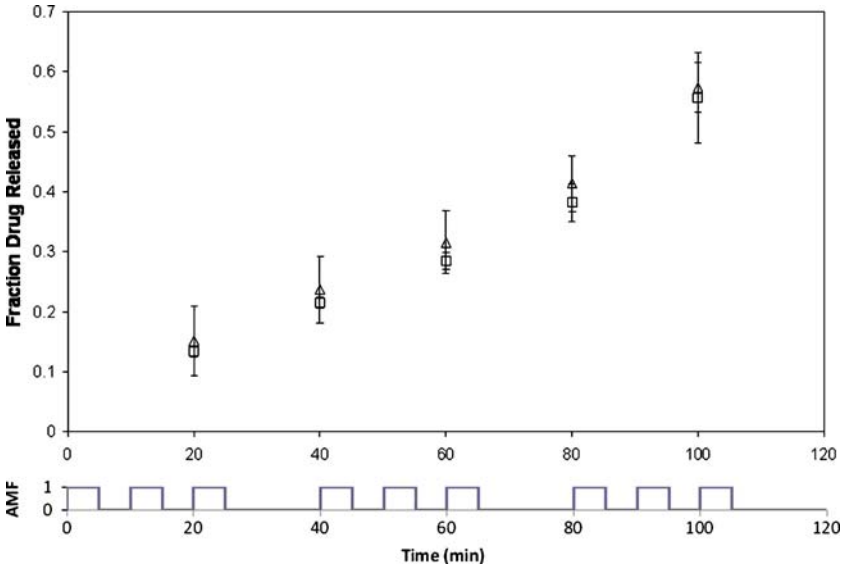

Fig. 7. Pure hydrogel drug release profile demonstrating no shift in the drug release graph upon AMF exposure. Pure control samples kept at 37°C (*triangle*), compared to the pure EMF exposed samples (*square*). *Lower graph* represents the field dosing schedule, *1* on, *0* off. $N=3\pm1$ standard deviation.

CONCLUSION

This study demonstrates the potential for external control over an implantable degradable biomaterial (*e.g.*, drug delivery device). The mechanism involves remotely heating nanoscale magnetic particles to increase the degradation rate of a degradable hydrogel and therefore increase the rate of drug release from the system. Though this hydrogel system degraded quickly and would not be applicable for *in vivo* application, longer degrading systems could be controlled by this mechanism as well.

ACKNOWLEDGEMENTS

This material is based in part on work supported by the National Science Foundation through an NSF IGERT traineeship and CTS-0609117 (NSF NIRT).

APPENDIX

Table I. Macromer Characterization

Macromer diacrylate to amine ratio	Number average molecular weight M_n	Weight average molecular weight M_w	Polydispersity index	Viscosity (cP) at 20.8°C
1.3	2,149	4,995	2.32	>instrument limit
1.6	1,494	3,427	2.29	231.1
2.0	1,036	2,108	2.034	28.3

Table II. Rate Constant and Activation Energy Values

Temperature (K)	k_{Pure} (mg/mL/min)	$k_{Particle}$ (mg/mL/min)	$1/T$ ($\times 10^{-3}$) ($1/K$)	$\ln(k_{Pure})$	$\ln(k_{Particle})$
298	0.010	0.008	3.36	−4.562	−4.812
310	0.020	0.016	3.23	−3.914	−4.113
328	0.038	0.035	3.05	−3.266	−3.350

Table III. Rate Constant and Activation Energy Values

Hydrogel system	E_a/R value (K)
Pure hydrogel	4,189
5 wt.% particle loaded hydrogel	4,736

REFERENCES

1. L. S. Nair, and C. T. Laurencin. Biodegradable polymers as biomaterials. *Prog. Polym. Sci.* **32**(8–9):762–798 (2007). doi:10.1016/j.progpolymsci.2007.05.017.
2. J. Kopecek. Smart and genetically engineered biomaterials and drug delivery systems. *Eur. J. Pharm. Sci.* **20**(1):1–16 (2003). doi:10.1016/S0928-0987(03)00164-7.
3. C. C. Lin, and A. T. Metters. Hydrogels in controlled release formulations: Network design and mathematical modeling. *Adv. Drug Deliv. Rev.* **58**(12–13):1379–1408 (2006). doi:10.1016/j.addr.2006.09.004.
4. K. R. Kamath, and K. Park. Biodegradable hydrogels in drug-delivery. *Adv. Drug Deliv. Rev.* **11**(1–2):59–84 (1993). doi:10.1016/0169-409X(93)90027-2.
5. N. A. Peppas, *et al.* Hydrogels in biology and medicine: From molecular principles to bionanotechnology. *Adv. Mater.* **18**(11):1345–1360 (2006). doi:10.1002/adma.200501612.
6. J. D. Kretlow, L. Klouda, and A. G. Mikos. Injectable matrices and scaffolds for drug delivery in tissue engineering. *Adv. Drug Deliv. Rev.* **59**(4–5):263–273 (2007). doi:10.1016/j.addr.2007.03.013.
7. L. G. Griffith. Polymeric biomaterials. *Acta. Mater.* **48**(1):263–277 (2000). doi:10.1016/S1359-6454(99)00299-2.
8. B. D. Ratner, and S. J. Bryant. Biomaterials: Where we have been and where we are going. *Annu. Rev. Biomed. Eng.* **6**:41–75 (2004). doi:10.1146/annurev.bioeng.6.040803.140027.
9. A. S. Sawhney, C. P. Pathak, and J. A. Hubbell. Bioerodible hydrogels based on photopolymerized poly(ethylene glycol)-co-poly(alpha-hydroxy acid) diacrylate macromers. *Macromolecules*. **26**(4):581–587 (1993). doi:10.1021/ma00056a005.
10. D. G. Anderson, *et al.* A combinatorial library of photocrosslinkable and degradable materials. *Adv. Mater.* **18**(19):2614–2618 (2006). doi:10.1002/adma.200600529.
11. D. M. Brey, I. Erickson, and J. A. Burdick. Influence of macromer molecular weight and chemistry on poly(beta-amino ester) network properties and initial cell interactions. *J. Biomed. Mater. Res. Part A*. **85A**(3):731–741 (2008). doi:10.1002/jbm.a.31494.
12. N. Harris, M. J. Ford, and M. B. Cortie. Optimization of plasmonic heating by gold nanospheres and nanoshells. *J. Phys. Chem., B*. **110**(22):10701–10707 (2006). doi:10.1021/jp0606208.
13. I. K. Tjahjono, and Y. Bayazitoglu. Near-infrared light heating of a slab by embedded nanoparticles. *Int. J. Heat Mass Transfer.* **51**(7–8):1505–1515 (2008). doi:10.1016/j.ijheatmasstransfer.2007.07.047.
14. R. A. Frimpong, S. Fraser, and J. Z. Hilt. Synthesis and temperature response analysis of magnetic-hydrogel nanocomposites. *J. Biomed. Mater. Res. Part A*. **80A**(1):1–6 (2007). doi:10.1002/jbm.a.30962.
15. N. S. Satarkar, and J. Z. Hilt. Hydrogel nanocomposites as remote-controlled biomaterials. *Acta. Biomaterialia*. **4**(1):11–16 (2008). doi:10.1016/j.actbio.2007.07.009.
16. N. S. Satarkar, and J. Z. Hilt. Magnetic hydrogel nanocomposites for remote controlled pulsatile drug release. *J. Control. Release*. **130**(3):246–251 (2008). doi:10.1016/j.jconrel.2008.06.008.
17. L. L. Lao, and R. V. Ramanujan. Magnetic and hydrogel composite materials for hyperthermia applications. *J. Mater. Sci., Mater. Med*. **15**(10):1061–1064 (2004). doi:10.1023/B:JMSM.0000046386.78633.e5.
18. R. Hergt, *et al.* Magnetic particle hyperthermia: nanoparticle magnetism and materials development for cancer therapy. *J. Phys., Condens. Matter.* **18**(38):S2919–S2934 (2006). doi:10.1088/0953-8984/18/38/S26.